Strain relaxation in small adsorbate islands: O on W(110)

T. O. Menteş,[1] N. Stojić,[2,3] N. Binggeli,[4,3] M. A. Niño,[1] A. Locatelli,[1] L. Aballe,[5] M. Kiskinova,[1] and E. Bauer[6]
[1]*Sincrotrone Trieste S.C.p.A., Basovizza-Trieste 34012, Italy*
[2]*Scuola Internazionale Superiore di Studi Avanzati (SISSA), Via Beirut 2-4, Trieste I-34014, Italy*
[3]*Theory @ Elettra Group, INFM-CNR Democritos, Trieste I-34014, Italy*
[4]*Abdus Salam International Centre for Theoretical Physics, Strada Costiera 11, Trieste 34014, Italy*
[5]*CELLS-ALBA Synchrotron Light Facility, C3 Campus Universitat Autónoma de Barcelona, 08193 Bellaterra, Barcelona, Spain*
[6]*Department of Physics, Arizona State University, Tempe, Arizona 85287-1504, USA*
(Received 29 January 2008; revised manuscript received 27 February 2008; published 9 April 2008)

The stress-induced lattice changes in a $p(1\times2)$ ordered oxygen layer on W(110) are measured by low-energy electron diffraction. We have observed that small oxygen islands show mismatch with the underlying lattice. Our results indicate that along $[1\bar{1}0]$, the average mismatch inversely scales with the island size as $1/L$ for all oxygen coverages up to 0.5 ML, while along [001], it is significant only for the smallest oxygen islands and scales as a higher power of the inverse island size. The behavior along $[1\bar{1}0]$ is described by a one-dimensional finite-size Frenkel–Kontorova model. By using this model, together with the calculated force constants, we make a quantitative estimate of the change in surface stress upon oxygen adsorption. The result is consistent with our *ab initio* calculations, which give a relative compressive stress of −4.72 N/m along $[1\bar{1}0]$ and a minute relative tensile stress of 0.15 N/m along [001]. The scaling along [001] is qualitatively explained as an effect induced by the lattice relaxation in the $[1\bar{1}0]$ direction.

DOI: 10.1103/PhysRevB.77.155414 PACS number(s): 61.05.jh, 68.43.Bc, 68.35.Gy

I. INTRODUCTION

The surfaces of solids present interesting phenomena because of their reduced dimensionality and nontrivial symmetry, with semi-infinite bulk on one side and vacuum on the other. From a simplified point of view, the charge freed by the absence of the vacuum side bonds has to be redistributed, resulting in major changes in the elastic,[1] magnetic,[2] and other thermodynamic[3] properties of the surface as compared to those of the bulk. Often, this results in structural modulations that minimize the energy and reduce the stress on the surface. On the other hand, adsorbates may induce similar effects, restructuring the surface at atomic or mesoscopic length scales.[1,4] Our study is based on such observations and aims at a better understanding of the elastic properties of adsorbate-covered crystal surfaces.

The determination of surface stress, which is central to the understanding of the self-organization processes on crystal surfaces, has proven to be a challenge. Especially, the few studies that compare experiment to theory do not provide a systematic level of agreement. Two such comparisons are on the changes in surface stress upon oxygen adsorption on Pt(111) (Refs. 1 and 5) and Cu(100).[6,7] In the first case, the calculation result is somewhat lower than the experimental one, whereas in the case of O/Cu(100), the theoretical values exceed the experimental results by a factor as large as 3. In a similar study, the calculation significantly underestimates the experiment on O/Ni(100).[8] The uncertainties are attributed to the sensitivity to the boundary conditions in the setup and the macroscopic nature of the measurement in the crystal-bending experiments, which is by far the most popular technique regarding adsorbate induced surface stress, and the lack of convergence in the density-functional theory (DFT) calculations. Therefore, additional means of measuring surface stress are very important.

To this end, one could consider the lattice relaxations upon stress release at a boundary. Strain relaxation in finite-size objects is not surprising because it is reasonable to expect that the boundaries (be it one dimensional or two dimensional) will assume a configuration minimizing the forces. Indeed, pioneering experimental studies regarding the change in the lattice constant of tiny three-dimensional crystallites were done in the early 1950s,[9] and somewhat later, the connection of this observation to surface stress was established.[10] In these studies, the contraction of small spherical metal crystals was explained through the radial forces applied by the surface to the inner part of the particles, laying out the basis for understanding our experimental observations.

Regarding surfaces, there is a wide range of studies on elastic effects due to a variety of defects such as single atoms, atomic steps, and three-dimensional adsorbate islands. Within the general framework, defects are modeled as local forces that induce long-range elastic relaxations on the surface and in the bulk (see Ref. 11 and references therein). The propagation of the displacements into the bulk has been most notably demonstrated by x-ray diffraction analysis.[12] However, the relevant interactions are often confined to the most superficial layers, as in the case of O adsorbed on Pt(110)-(1×2).[13]

Following this argument, to a first approximation, an adsorbate island can be considered as a two-dimensional crystallite with a one-dimensional boundary. In the case of pseudomorphism, the adsorbate lattice locks on to that of the underlying crystal. However, for small monolayer islands, the stressed layer might be able to, at least partially, relax through its boundaries, and we can expect mismatch between the adsorbate and the substrate. There is already experimental work pointing to such relaxations both on metals and on semiconductors by using real space imaging and diffraction

techniques.[13–16] On the theoretical side, recent simulations show deviations from pseudomorphic positions for small two-dimensional islands.[17,18]

In this paper, we demonstrate that quantitative information on surface stress can be obtained by measuring such deviations from pseudomorphism as a function of the size of the monolayer adsorbate islands. We observe that small islands of oxygen on W(110) behave similarly to the cases mentioned above, showing mismatch to the underlying lattice a_0 depending on their size and the crystallographic direction within the surface plane. By taking advantage of the distinct low-energy electron diffraction (LEED) spots corresponding to the $p(1\times2)$ order, we follow the changes in the average lattice spacing as a function of the average domain size obtained from the spot widths. We find a mismatch scaling as the inverse island size, $1/L$, in the $[1\bar{1}0]$ direction, while it is dominated by quadratic and higher-order terms, $O((a_0/L)^2)$, along [001]. The lattice mismatch is explained as a strain relaxation, and it is described in terms of a Frenkel–Kontorova model. From this model, by using calculated force constants, we extract the surface-stress value along $[1\bar{1}0]$.

Furthermore, we have performed DFT calculations to understand the nature of the oxygen-induced surface-stress change, which was obtained by modeling the observed strain relaxations in our measurements. While the early first-principles surface-stress calculations[19,20] were mostly oriented toward the understanding of the microscopic origin of stress, some of the more recent ones[5,6,8] are being directly compared to the experimental measurements of the surface-stress change, with varying success. Our *ab initio* result agrees well with the stress value estimated from our model of the measured lattice relaxations in the $[1\bar{1}0]$ direction. In addition, the qualitatively different scaling of the lattice mismatch along [001] can be understood from our calculation results, which show lack of a significant stress change in this direction and a strain-stress coupling between the two orthogonal directions. The latter is expected to give rise to a $(1/L)^2$-like scaling along [001], which is induced by the strain relaxation in $[1\bar{1}0]$.

The paper is organized as follows. Section II describes the experimental setup and reports the LEED results on oxygen adsorption on W(110), Sec. III presents the model of lattice relaxation as a balls-and-springs chain, and Sec. IV describes the *ab initio* calculations. Section V presents and compares the results of our model to those of our DFT calculations along with a discussion involving the available experimental and theoretical work on W(110).

II. EXPERIMENT

A. Setup

The microspot low-energy electron diffraction (μ-LEED) measurements were performed with the SPELEEM microscope in operation at Elettra, Italy.[21] The instrument combines a variety of techniques including μ-LEED and low-energy electron microscopy (LEEM). The specimen is illuminated with an electron beam generated by a LaB_6 gun (energy width of ~0.6 eV) at a flux density of less than 10^{-2} nA/m^2. In the LEED operation mode, the microscope images the diffraction pattern produced by the sample at the back focal plane of the objective lens.[22] The probed area on the surface is selected by inserting an aperture that defines an incident electron beam of 2 μm diameter.

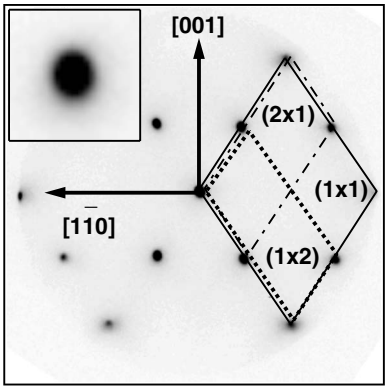

FIG. 1. The $p(1\times2)$ LEED pattern corresponding to 0.5 ML oxygen on W(110). The crystallographic directions are marked on the figure. Note the presence of both (1×2) and (2×1) domains. A blowup of the $(0,-1/2)$ spot is shown in the inset.

Prior to the μ-LEED measurements, a microregion with a single monatomic W step was chosen using the LEEM mode to avoid the broadening of the diffraction peaks due to step bunches. The reciprocal space calibration and the measurement of the transfer width of the instrument were performed in such a region of the clean unreconstructed (1×1) W surface. We determined an instrument transfer width of about 110 Å at 30 eV electron energy.

The W(110) crystal was cleaned by annealing at 1000 °C in 2×10^{-6} mbar oxygen and subsequent high temperature flashes in ultrahigh vacuum to remove oxygen. The base pressure of the experimental chamber was 2.5×10^{-10} mbar. During the high temperature flashes, the pressure remained below 3×10^{-9} mbar. The sample was checked by using LEEM and LEED to confirm the absence of tungsten carbides forming on the surface.

To form the adsorbed oxygen phases, molecular oxygen was dosed by using a precision leak valve at a partial pressure of 5×10^{-9} mbar, as measured by an ion gauge. During the dosing, the LEED pattern was acquired every 20 s, with the sample kept at 450 K. An electron energy of 30 eV was used for the diffraction measurements, corresponding to the intensity maximum of the half-order spots of the $p(1\times2)$ structure. For the oxygen pressure used, the best $p(1\times2)$ order was obtained upon exposure of about 4.5 L, which corresponds to 0.5 ML oxygen coverage. The resulting LEED pattern is displayed in Fig. 1.

B. Low-energy electron diffraction measurements

The adsorption of oxygen on W(110) has been thoroughly investigated in the past.[23] It is well known that for coverages below 0.5 ML, oxygen can be found in islands with $p(1\times2)$ order, which evolves into $p(2\times2)$ and (1×1) reconstructions with increasing oxygen coverage.[24] In spite of

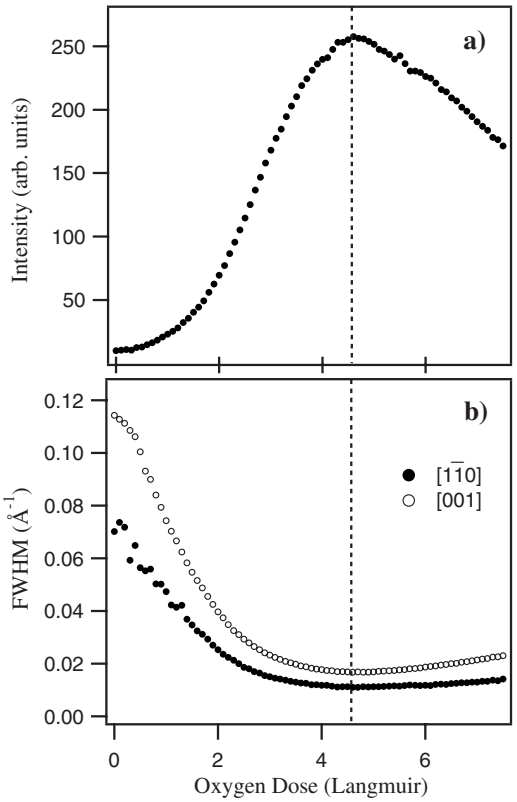

FIG. 2. The intensity and the FWHM of the $p(1\times2)$ spots are given as a function of the oxygen dose. The instrumental transfer width is taken into account for the FWHM values. The dashed line corresponds to 0.5 ML oxygen coverage.

the stress induced by the oxygen layer, the effective attractive interactions between the oxygen atoms manage to stabilize the ordered islands even at very low oxygen coverages (note that effective interactions include attractive nearest neighbor, repulsive next-nearest neighbor of similar magnitude, and attractive but weaker third-nearest neighbor[25]).

Figure 2 shows the evolution of the intensity and width of the $p(1\times2)$ half-order spots during oxygen uptake at 450 K. In agreement with the literature, even at the lowest coverages, we can identify diffuse $p(1\times2)$ spots, which grow in intensity and become sharper upon further exposure to oxygen. As seen in Fig. 2, the $p(1\times2)$ intensity maximum at 4.5 L corresponds to a minimum of the spot widths. Above this coverage, the $p(1\times2)$ domains break up due to additional oxygen atoms filling in the missing oxygen rows, which results in a slight broadening of the spots. Interestingly, the half-order spot width along $[1\bar{1}0]$ is always smaller compared to that along [001] by roughly a factor of $\sqrt{2}$, pointing to oxygen islands elongated in the $[1\bar{1}0]$ direction. Beyond 0.5 ML, a weak $p(2\times2)$ order appears, which develops very slowly due to the drop in the oxygen sticking coefficient with increasing coverage.[23]

In the analysis of the half-order spot profiles, both Gaussian and Lorentzian fits were used to extract the full width at half maximum (FWHM) values and the spot positions. A slowly varying background was subtracted as a low order polynomial. At high coverages, close to 0.5 ML, the peak shapes are predominantly Gaussian with a weak Lorentzian tail, whereas at the lowest coverages, both fits gave equally good results. The Lorentzian tail at higher coverages is consistent with the results of Wu *et al.*,[25] which point to a bimodal island-size distribution. Nevertheless, for simplicity, we will consider only the mean value of the size distribution extracted from the width of the dominant Gaussian contribution.

Beyond the established behavior of oxygen on W(110), we have observed a new effect manifested in the $p(1\times2)$ spot separations. By following the evolution of the oxygen unit cell as a function of oxygen coverage, we noticed deviations of the reciprocal space vectors from those expected from the underlying tungsten lattice. The mismatch of the oxygen $p(1\times2)$ unit cell to the tungsten lattice is displayed in Fig. 3. The fractional differences are plotted against the average *domain size*, which is obtained from the FWHM values plotted in Fig. 2(b). The variations are larger for low oxygen coverages, which also correspond to larger FWHM values of the half-order spots. We note that at low coverages, the oxygen lattice expands along $[1\bar{1}0]$ and shrinks along

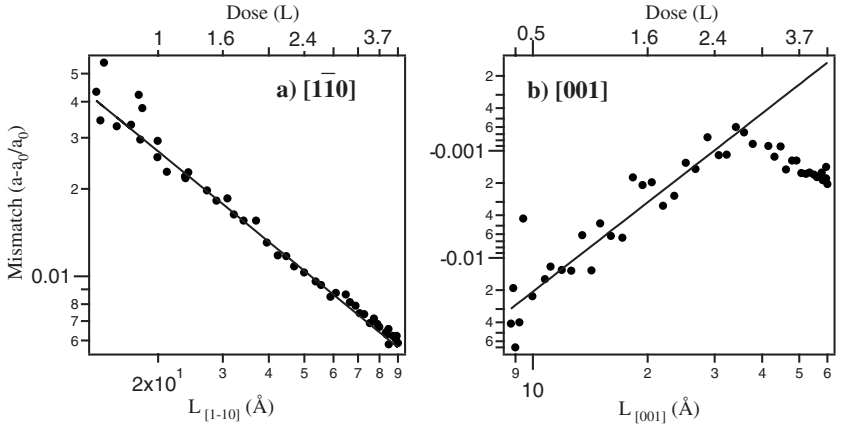

FIG. 3. The changes in the $p(1\times2)$ oxygen lattice spacing along $[1\bar{1}0]$ and [001] are shown as a function of the average dimension of the (1×2) domains. The filled circles are the data extracted from the LEED measurements, and the lines are power law functions fitted to the data. Both axes are given in logarithmic scale. The mismatch values are referenced to the W lattice. The domain sizes are found from the full width at half maximum of the diffraction spots. Note that the data are shown up to an oxygen coverage of 0.5 ML.

TABLE I. Results of the power law fit to the data in Fig. 3. The definition of parameters A and p is given in Eq. (1).

Direction	A (Å^p)	p
$[1\bar{1}0]$	0.56 ± 0.05	1.04 ± 0.05
[001]	-0.78 ± 0.21	2.77 ± 0.29

[001]. The magnitude of the mismatch to the tungsten lattice is roughly an order of magnitude larger along $[1\bar{1}0]$, except at the lowest oxygen coverages for which the $p(1\times2)$ LEED spots are barely visible.

The power law dependence of the mismatch on the domain size is clear from the linear trend in the log-log plots in Fig. 3. The solid lines correspond to a fitting function of the following kind:

$$\frac{a_{\text{meas}}(L) - a_0}{a_0} = \frac{A}{L^p}, \tag{1}$$

where the left hand side corresponds to the measured average fractional mismatch of the oxygen lattice with respect to the W(110) surface. L is the linear size of the oxygen island along the direction of interest, and A and p are the two parameters used to fit the data. The parameters resulting from the fit are displayed in Table I.

As seen in Table I, along $[1\bar{1}0]$, the fractional lattice mismatch inversely scales with the linear dimension L ($p=1$). Along [001], instead, the inverse-scaling power indicates a relaxation dominated by higher-order terms, i.e., $O((a_0/L)^n)$, with $n \geq 2$. Leaving the discussion to the following sections, here, we limit ourselves to mention that this points to a qualitative difference in the driving force of the strain relaxation along the two directions. Apart from the scaling power, the particular value of parameter A carries more information specific to the adsorbate-substrate interactions, especially along $[1\bar{1}0]$, as we will show in Sec. III.

In Fig. 3(b), we note that at $L_{[001]} \simeq 32$ Å (corresponding to an oxygen dose of 3 L and a coverage of 0.4 ML), the lattice along [001] stops expanding and starts shrinking. The likely origin of this abrupt change is the onset of "island percolation" or the touching of the ordered islands.[23] A kink is also present in Fig. 3(a) at $L_{[1\bar{1}0]} \simeq 60$ Å, which roughly corresponds to the same coverage. However, the effect is more evident in Fig. 3(b) due to the small magnitude of the fractional mismatch along [001].

III. MODELING STRAIN RELAXATION

By assuming that lattice relaxation in finite-sized objects is limited to the boundaries, one would expect that the average lattice spacing should converge to a fixed value (to the bulk value for three-dimensional crystals or to the underlying lattice for a two-dimensional pseudomorphic film), and that the difference from the bulk lattice should be inversely proportional to the object size. This statement is independent of the dimensionality because the bulk divided by the boundary always gives the linear dimensions of the system. The idea can be formulated through a fractional mismatch:

$$\epsilon \equiv \frac{a(L) - a_0}{a_0} \propto \frac{1}{L}, \tag{2}$$

where L is the linear dimension along the direction under study, and a_0 is the lattice constant expected from an infinite object. One can safely assume that this simple scaling argument holds for larger objects. However, at the limit of a few atoms, this is not necessarily the case because the interactions giving rise to stress may be modified due to finite-size effects.[18]

Keeping this in mind, we note that for O/W(110), the average relaxation along $[1\bar{1}0]$ scales as $1/L$ all the way down to the smallest linear dimensions. Indeed, inverse scaling is represented by the solid line in Fig. 3(a), which follows the experimental points throughout the full range of domain sizes. The expansion of the oxygen lattice along $[1\bar{1}0]$ for the islands can be explained by the large compressive stress in this direction from our *ab initio* calculation for the $p(1\times2)$-O/W(110) surface, as we will show in Sec. V. The oxygen layer is compressed to match the W lattice along $[1\bar{1}0]$, and at the boundary of islands, it relaxes the compression by expanding.

The almost perfect inverse scaling in the measurements encourages one to extract quantitative information from the data using a simplified model. The information specific to the system under study is coded in the proportionality factor in Eq. (2), which we had termed as A earlier in Sec. II. Having access to a single experimental coefficient, we will make a set of assumptions in order to reduce the number of parameters in the model problem:

(i) The displacements due to strain relaxation are assumed to be limited to the oxygen layer, with the tungsten atoms fixed.

(ii) The $[1\bar{1}0]$ direction is treated independently of [001].

(iii) The stress difference (across the island boundary) is assumed to be manifested as a point force at the island boundary within the surface plane.

The first assumption is a drastic one and is expected to introduce the largest errors in the quantitative prediction of the model. Previous structural studies assumed that the topmost tungsten layer preserves the atomic positions of the clean W(110) surface when covered with the (1×2)-O layer,[26,27] pointing to the rigidity of the substrate, which provides the basis for our assumption. However, the results of our DFT calculations, to be summarized in Sec. IV, show that the W atomic positions are slightly modified both laterally and along the surface normal upon oxygen adsorption.

The second statement, on decoupling $[1\bar{1}0]$ from [001], is valid due to the small magnitude of oxygen-induced surface-stress change along [001]. This assumption leads to a reduction (or projection) in the surface, which can be understood from Fig. 4. The "W" and "O" atoms on the side view of the surface can be regarded as effective particles corresponding to a line of atoms along [001]. The force constants (describing the interactions at the harmonic limit) along $[1\bar{1}0]$ be-

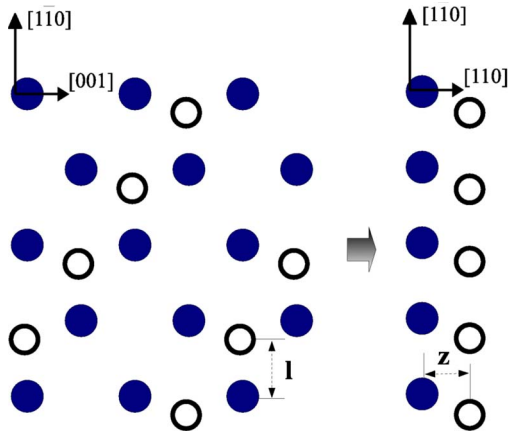

FIG. 4. (Color online) The top and side views of a $p(1\times2)$-O covered area on W(110). Oxygen (tungsten) atoms are represented by the empty (solid) balls. The two parameters describing the position of oxygen atoms, z and l, are marked on the figure.

tween these effective atoms are defined by infinitesimal movements of the corresponding line of atoms as a whole.

In the third assumption, we replace the net force distribution at the island boundary by a point force proportional to the difference in surface stress inside and outside the islands.[11,12] The resulting model for the adsorbate island is shown in Fig. 5. The interactions between the oxygen atoms are sketched as springs, whereas the effect of the tungsten substrate on the oxygen atoms is shown as a periodic potential profile. Therefore, we have reduced the problem to that of a one-dimensional finite-size Frenkel–Kontorova chain.[28] Within such a model, only the nearest-neighbor interactions are considered. We will make an additional assumption accounting for all interactions going beyond the nearest neighbors into an effective spring constant.

The relevant parameters in our model can be seen in Fig. 5. The substrate potential is defined by its period a_0 and a force constant k_0. The oxygen-oxygen bonds are modeled as springs, with an equilibrium length a_1 and a spring constant k_1. The relaxation of the oxygen-oxygen springs in the presence of the boundary is given by the distance of the i^{th} oxygen atom to the i^{th} adsorption site, which we denote as Δx_i. By assuming harmonic interactions, the total energy of a $(2N+1)$-atom adsorbate chain is

$$E_{\text{tot}} = 2\sum_{i=1}^{N} \frac{1}{2}k_0(\Delta x_i)^2 + 2\sum_{i=1}^{N} \frac{1}{2}k_1[a_1 - (a_0 + \Delta x_i - \Delta x_{i-1})]^2, \tag{3}$$

where we have assumed symmetry around the center with the center atom fixed ($\Delta x_{i=0}=0$). The positions in the ground state are found by setting the net force on each atom to zero ($\partial E/\partial x_i=0$).

The fractional mismatch of the adsorbate chain to the substrate can be expressed as

$$\epsilon = \frac{\Delta x_N - \Delta x_{-N}}{L} = \frac{2\Delta x_N}{L}, \tag{4}$$

where the length of the chain is $L=(2N+1)a_0$. The second

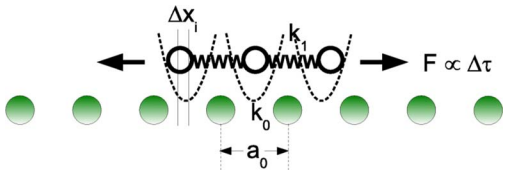

FIG. 5. (Color online) The sketch of the side view of an oxygen island on the W surface. The oxygen atoms are denoted with empty circles, and the first layer tungsten atoms are shown as solid balls. The effect of the tungsten surface on the adsorbate layer is represented by a periodic potential profile with parabolic potential wells.

equality is due to symmetry. From a comparison of Eqs. (1) and (4), we see that $A=2\Delta x_N$. In other words, the coefficient of the power law is directly related to the displacement of the boundary atoms.

Although the statement of the problem looks simple, a general analytical solution is surprisingly difficult to find. Instead, it is possible to approximate the solution for the mismatch:

$$\epsilon = -\frac{2F}{f(k_0,k_1)}\frac{1}{L} + O\left[\left(\frac{a_0}{L}\right)^2\right], \tag{5}$$

where $f(k_0,k_1)$ is a function which can be numerically evaluated (see the Appendix). It can be approximated as $f(k_0,k_1) = k_0 + ck_1$, where c is a factor of the order of unity, which depends on the ratio of the force constants ($c\approx1$ for $k_0 \gg k_1$). F is the net force on the boundary atom, which corresponds to the change in the stress across the boundary. The higher-order terms on the right contribute only for very small island sizes, $L<4a_0$, above which they are negligible. As expected for a one-dimensional system, the unit of stress is that of force. The connection to the actual stress on the two-dimensional surface along the direction of the chain can be established by

$$F = a_{0\perp}\Delta\tau, \tag{6}$$

where $a_{0\perp}$ is the unit length (defined per atom) along the perpendicular direction, and $\Delta\tau$ is the change in the actual surface stress across the island boundary. We note that in this model, F and $\Delta\tau$ do not depend on L, which is consistent with an experimental $1/L$ scaling of ϵ. Hence, $\Delta\tau$ corresponds to the macroscopic surface stress induced by the chain in the asymptotic limit ($L\to\infty$). By putting together Eqs. (5) and (6), we obtain the measured coefficient as

$$A = -\frac{2a_{0\perp}\Delta\tau}{f(k_0,k_1)}, \tag{7}$$

which, in essence, states that the movement of the boundary atom is proportional to the net force on it and is inversely proportional to the steepness of the potential well in which the atom is sitting. Through this expression, we have a means of relating the experimentally measured power law coefficient A to the macroscopic surface stress.

In the next sections, we will combine the results of this model with those from our *ab initio* calculations. In particular, we will evaluate the microscopic force constants k_0 and k_1 from the DFT calculations. We will then compare the

TABLE II. Tungsten relaxations for the two topmost layers, which are given in percentage of the bulk lattice constant, as obtained in various calculations and the experiment.

	Δd_{12} (%)	Δd_{23} (%)
Our LDA result	−3.6	0.2
Arnold *et al.*[a]	−3.6	0.2
Qian and Hübner[b]	−4.1	−0.4
Batirev *et al.*[c]	−0.8	0.3
Ackland and Finnis[d]	−1.2	0
Experiment[a]	−3.1	0

[a]Reference 33.
[b]Reference 34.
[c]Reference 35.
[d]Reference 36.

resulting stress from Eq. (7) to the macroscopic surface stress obtained from the first-principles calculations.

IV. *AB INITIO* CALCULATIONS

We have performed DFT pseudopotential calculations in a plane-wave basis by using the PWSCF code.[29] The surface stress was analytically calculated on the basis of the expression derived by Nielsen and Martin,[30] which is based on the Hellmann–Feynman theorem, and following Ref. 19. We utilized a symmetric slab with 13 layers to simulate the W surface and 15 layers for O/W, with 9 vacuum layers, for both relaxations and subsequent stress calculations. We used the local-density approximation (LDA) in the Perdew–Zunger parametrization[31] for exchange and correlation and employed Vanderbilt ultrasoft pseudopotentials[32] generated from the $2s^2 2p^4$ atomic configuration of oxygen and $5s^2 5p^6 5d^4 6s^2$ configuration of tungsten. The pseudopotential core-cutoff radii for O were $r_{s,p}=1.6$ and $r_d=1.4$ a.u. and for W, they were $r_{s,p}=2.2$ and $r_d=2.4$ a.u. Our kinetic energy cutoff was 35 Ry for the wave functions and 350 Ry for the charge density. We used 326 k points in the irreducible Brillouin zone. The forces were converged to better than 1.7 mRy/Å.

As a prerequisite for the surface-stress calculations, we relaxed the positions of the atoms in the W slab, keeping the central three layers fixed. Table II shows our results for the out-of-plane relaxations of the two topmost layers of a clean W slab together with the available data from the literature. The theoretical results of Arnold *et al.*[33] are for a nine-layer slab, calculated with an all-electron method using the LDA. Qian and Hübner,[34] within the same method, used a five-layer slab and the generalized gradient approximation for exchange and correlation. Similarly, Batirev *et al.*[35] applied a modified linearized augmented plane wave (LAPW) method with LDA to a five-layer W slab. On the other hand, Ackland and Finnis[36] utilized a semiempirical model with parametrized energy functions. We note good agreement between our results, the experiment, and the previous *ab initio* calculation on a slab of sufficient size,[33] while the five-layer slabs were too small and the semiempirical model[36] gave a rather poor result in comparison with experiment.

TABLE III. Position of the oxygen atom after relaxing the slab. The first column shows the W bulk lattice constant. z_1 and z_2 denote the vertical distance of the oxygen atom to the two inequivalent tungsten atoms with one and two oxygen neighbors, respectively.

	a_{bulk} (Å)	l/a	z_1/a	z_2/a
Our result	3.14	0.52	0.38	0.36
Załuska-Kotur *et al.*[a]	3.00	0.56	0.43	0.43
Experiment[b]	3.16	0.53	0.40	0.40

[a]Reference 37.
[b]Reference 27.

Similarly, we relaxed the atomic positions in the tungsten slab with adsorbed oxygen in the $p(1\times2)$ reconstruction. Figure 4 gives the top and side views of the $p(1\times2)$-O/W(110) surface and defines the parameters l and z, which describe the position of the oxygen atom. The results of the calculation corresponding to these positional parameters are given in Table III. There, the l and z displacements in the $p(1\times2)$ reconstruction are shown for the relaxed slab with reference to the calculated W bulk lattice constant, which is given in the first column. For comparison, the quantum-mechanical DFT calculation of Załuska-Kotur *et al.*[37] using the atomic-cluster approach with only one O atom is also included in the table. As evidenced by the bulk lattice constant, the cluster method gives a considerably compressed structure. On the other hand, there is excellent agreement between our calculation and the experimental results based on LEED measurements, especially regarding the W lattice constant and the lateral displacement of the oxygen atom. In terms of layer spacings, the LEED $I(V)$ analysis[27] did not allow any out-of-plane movement of the substrate atoms upon oxygen adsorption, while our relaxed positions indicate an ~0.05 Å buckling of the outermost plane of W atoms due to the oxygen atoms. This result is consistent with an original estimate of up to 0.05 Å for the out-of-plane displacement due to oxygen adsorption.[38] Additionally, the O atom in our calculation is displaced in the [001] direction by less than 0.05 Å, which was also not taken into account in the LEED model of Ref. 27. We note that this rigid displacement of the whole adsorbate layer along [001] is allowed because it does not violate any symmetry operation on the surface.

V. SURFACE STRESS AND LATTICE RELAXATION

In order to obtain an estimate of $\Delta\tau$ along $[1\bar{1}0]$ from the strain-relaxation measurements by using Eq. (7), we have evaluated the force constants from the *ab initio* slab calculation described in Sec. IV by infinitesimally moving the atoms and following the change in energy. The parameter k_0, which corresponds to the on site potential profile felt by the oxygen atoms, was found to be $k_0=8.6$ eV/Å^2 by rigidly sliding the oxygen layer over the surface.[39] Similarly, the oxygen-oxygen force constant was obtained to be $k_1\approx0.6$ eV/Å^2 by moving every other oxygen atom along $[1\bar{1}0]$ and taking into account the additional energy increase due to the substrate potential (the total energy increase is proportional to k_0

TABLE IV. The results of our surface-stress calculations and of the relative stress between the O/W(110) and W(110) surfaces. For comparison, in the last two columns, we give the surface stress change obtained from our LEED analysis and that from a previous experiment using the crystal-bending method (Ref. 42). The values are all given in N/m. The positive sign corresponds to the tensile stress.

Direction	$\tau^{\mathrm{DFT}}_{W(110)}$	$\tau^{\mathrm{DFT}}_{p(1\times2)\text{-O/W}(110)}$	$\Delta\tau^{\mathrm{DFT}}$	$\Delta\tau^{\mathrm{LEED}}$	$\Delta\tau^{\mathrm{a}}$
$[1\bar{1}0]$	3.58	−1.14	−4.72	−6.5	−1.1
[001]	5.26	5.41	0.15		−0.1

[a]Reference 42.

$+2k_1$). The small value of k_1 with respect to k_0 is expected, because the weak oxygen-oxygen nearest-neighbor interactions are further reduced by the next-nearest-neighbor interaction of opposite sign and similar magnitude.[25] By taking the unit length along [001] as $a_{0\perp}=6.33$ Å and the measured coefficient $A=0.56$ Å, we obtain the oxygen-induced change in the surface stress along $[1\bar{1}0]$ to be $\Delta\tau^{[1\bar{1}0]}=-6.5$ N/m from Eq. (7).

We present our surface-stress results from *ab initio* calculations on clean W(110) and on $p(1\times2)$-O/W(110) in the first two columns in Table IV. The difference of the two, which is the oxygen-induced surface-stress change, is listed in the third column. The numerical uncertainty of the calculated LDA surface stress is estimated to be 0.36 N/m based on convergence checks in which we increased the energy cutoffs and the number of k points. To further check our results, we calculated the surface stress from the total energy difference for two strains with a magnitude of 1.5% and opposite signs (i.e., contraction and expansion of the lattice constant along the $[1\bar{1}0]$ direction), which is based on the energy expansion to the second order in the strain (see Refs. 40 and 41). By this method, we obtained a relative surface stress in the $[1\bar{1}0]$ direction $\Delta\tau=-4.68$ N/m, which agrees very well with our analytical result.

The calculated surface stresses along $[1\bar{1}0]$ and [001] of the clean W(110) surface are both tensile. This is in qualitative agreement with the previous theoretical estimates.[35,36] We note, however, that our surface-stress values are larger than the average surface stress of 2.7 N/m obtained from a previous LDA calculation, in Ref. 35, for a five-layer slab. Aside from having the correct atomic structure, stress values do converge much slower with the number of k points than energies in the DFT calculations, and the long-ranged elastic relaxations bring forth the necessity for larger slabs, which is the motivation behind the rather thick slabs used in our calculations. The semiempirical potential calculations[36] yield, instead, surface stresses of 2.4 N/m along $[1\bar{1}0]$ and 0.3 N/m along [001], which significantly differ from the present *ab initio* results. Apart from the method, the difference is also from the poor structural optimization obtained in the empirical potential approach. To the best of our knowledge, no experimental data are available for the clean W(110) surface stresses. However, experimental values do exist for a related quantity that contributes to the surface stresses: the surface energy.[19] Our calculated surface energy of 3.5 J/m^2 is within the range of the available experimental data, 2.8–3.7 J/m^2.[43]

As for the oxygen-induced change in the surface stress, the crystal-bending data[42] have the same sign but they considerably differ in magnitude from our result. As seen in Table IV, both our calculation and the crystal-bending measurement show that the relative stress is compressive along $[1\bar{1}0]$, while along [001], the surface stress is negligibly affected upon oxygen adsorption. On the other hand, the surface-stress change that we obtained by modeling the average lattice relaxation as a function of island size, $\Delta\tau^{[1\bar{1}0]}=-6.5$ N/m, agrees well with the value of −4.72 N/m from the calculation, especially by considering the few parameters used in our model.

The reason for the remaining difference between the quantitative estimate from the model chain and the calculated stress is mainly attributed to the simplifications of the model itself. Most importantly, we have only considered the relaxations within the oxygen layer. As hinted by the modified tungsten atomic positions in the presence of oxygen, the relaxations in the adsorbate layer should continue into the tungsten surface, although with reduced magnitude. Thus, a more accurate model should take into account layer-resolved stresses, with the lattice in each layer (namely, oxygen and the first layer tungsten) having a different power law behavior (both with $p=1$ but each with a different coefficient A). Although possible, this would require a more precise measurement and a detailed analysis of the LEED spot profiles.

A quantitative comparison between the *ab initio* calculations and the crystal-bending results from Table IV is less satisfactory because the calculation is a factor of 4 above the experimental value along $[1\bar{1}0]$. Although discouraging, this illustrates the problems in the surface-stress studies. One problem noted in the mentioned experimental study is the adsorption of oxygen also on the back side of their crystal, which should result in the reduction in the measured stress by about 25%.[42] In addition, as suggested in Sec. I, part of the reason for the difference between experiment and theory is to be sought in the macroscopic nature of the crystal-bending measurements since the presence of domain boundaries relieves the stress on the adsorbate-covered surface. Indeed, our LEED analysis shows that even at 0.5 ML oxygen coverage, which corresponds to the best $p(1\times2)$ order, the oxygen lattice is relaxed along $[1\bar{1}0]$ by as much as 0.5%. At room temperature, this relaxation should be more pronounced because of the smaller domain sizes. As a consequence, the surface stress in the adsorbed face of the crystal is lower than the value estimated from a calculation that considers a surface uniformly covered and free of defects. The surface quality of the crystal used in the experiments can also influence the results, as the surface stress would be reduced by the presence of defects such as steps or step bunches. This problem was avoided in our μ-LEED measurements by choosing a region free of atomic steps.

Regarding the strain-relaxation processes, we have demonstrated that the behavior along $[1\bar{1}0]$ is consistent with what is expected from a harmonic chain sitting on a periodic potential. However, along [001], the situation presents a

qualitative difference as the power (with which the relaxation inversely scales as a function of island size) is much larger than 1 throughout the full range of oxygen coverages. Additionally, the mismatch along [001] is much smaller than that along $[1\bar{1}0]$ except for the smallest island sizes (see Fig. 3). As we have noted earlier, these observations suggest that the lattice relaxation along [001] is a consequence of the $[1\bar{1}0]$ relaxation, yielding a higher-order effect in a_0/L. Indeed, as seen in Table IV, our calculations predict no noticeable difference between the clean and oxygen-covered W(110) surface stresses in the [001] direction. We suggest that the lattice change along [001] is induced by the strain relaxations taking place in the $[1\bar{1}0]$ direction for small-sized islands. We find support for this explanation when we extend the calculation to a slab that is slightly stretched along $[1\bar{1}0]$ to model the strain relaxation. In particular, we have performed a calculation for a slab stretched uniaxially by 1.5% along $[1\bar{1}0]$. In this case, the differences in the surface stress with and without the oxygen on the surface were found to be $\Delta\tau^{[1\bar{1}0]}=-3.98$ N/m and $\Delta\tau^{[001]}=+0.68$ N/m.[44] As expected, along $[1\bar{1}0]$, the relative stress decreases as the compressed lattice relaxes upon stretching. On the other hand, along [001], a tensile stress appears as the lattice is stretched in the orthogonal direction. This strain-stress coupling between the two directions is therefore believed to be the driving force of the lattice changes along [001].

A similar analysis as in Eq. (2) can give us more insight into the power law behavior observed along [001]. If the driving force is the relaxation along $[1\bar{1}0]$, the regions in which the contraction in [001] occurs must be limited to what can be described as the "corners" of an island. It follows that there is an inverse relationship in the relaxation along [001] with the island area,

$$\epsilon_{[001]} \propto \frac{1}{L^2}. \tag{8}$$

The tendency of the strain relaxation ϵ to decay faster along [001] compared to $[1\bar{1}0]$ supports this argument. However, the difference between the measured inverse power $p=2.76$ (see Table I) and the estimated inverse square relationship along [001] is statistically significant. One issue that we have ignored in the discussion of the spot profiles and relaxations is related to the island-size and shape distributions. In general, the boundaries of oxygen islands do not run simply along $[1\bar{1}0]$ and [001]. Scanning tunneling microscopy studies of low oxygen coverages show a variety of island shapes possibly elongated in the $\langle 1\bar{1}1\rangle$ directions.[24] However, from our two-dimensional LEED spot profiles, we were able to determine only a mean elongation along $[1\bar{1}0]$. In addition to the shape, the details of the island-size distribution depend on the oxygen coverage.[25] It is plausible that a coverage dependent change in the asymmetry of this distribution would modify the power law of the apparent (or mean) strain relaxation.

VI. CONCLUSION

We have measured the lattice relaxations within oxygen islands on W(110) by low-energy electron diffraction. The half-order diffraction spots of the $p(1\times 2)$ structure within the oxygen-covered regions allowed the observation of the mismatch to the substrate lattice as a function of the average island size. Along $[1\bar{1}0]$, the mean lattice mismatch was shown to scale as the inverse island size, $1/L$, while along [001], the scaling involved a higher power of the inverse island size. We analyzed the inverse-scaling behavior along $[1\bar{1}0]$ through a finite-size balls-and-springs chain to estimate the oxygen-induced surface-stress change. The result is in fair agreement with our density-functional theory calculation. In addition, the calculations gave a small tensile stress along [001], which increased upon relaxing the compressive strain along $[1\bar{1}0]$. This provides support to our explanation that the qualitatively different behavior in the [001] direction is an effect induced by the lattice relaxation along $[1\bar{1}0]$.

We believe that with a more sophisticated analysis of the integral order LEED spot profiles, the semiquantitative strain-relaxation model described in this paper can be generalized to study the surface stress in a wide range of adsorbate systems and ultrathin films.

Note added. Recently, we became aware of an article[45] reporting *ab initio* calculations of surface stress in a few adsorbate systems, including O/W(110). There is good agreement between the surface-stress values of this article and ours.

APPENDIX

The derivation of Eq. (5) follows from setting the net force on each atom to zero in the Frenkel–Kontorova chain. By setting $\partial E/\partial x_i=0$ (for $i=0,\ldots,N$), we have

$$(k_0+2k_1)\Delta x_i = k_1(\Delta x_{i-1}+\Delta x_{i+1}) \quad \text{for} \quad i<N,$$

$$F+(k_0+k_1)\Delta x_N = k_1\Delta x_{N-1} \quad \text{for} \quad i=N, \tag{A1}$$

where F is the net force due to the stress change in the boundary atom ($i=N$) before the relaxations, Δx_i, balance it. To find the displacements, we have to simultaneously solve these $N+1$ equations. Instead of tackling the difficult task of finding a general analytic solution, we can make the assumption that only a few atoms from the boundary are significantly displaced. The result has the form

$$\Delta x_N = -\cfrac{F}{k_0+k_1-\cfrac{k_1^2}{k_0+2k_1-\cfrac{k_1^2}{k_0+2k_1\cdots}}} = -\frac{F}{f(k_0,k_1)}, \tag{A2}$$

where the last step defines the function $f(k_0,k_1)\approx k_0+ck_1$. Independently, we numerically solve the problem by recursively moving the atoms until all the forces vanish. A comparison of Eq. (A2) with the numerical solution gives a good agreement when we allow displacement of up to four atoms from the boundary. The average mismatch in Eq. (5) directly follows from Eqs. (4) and (A2).

[1] H. Ibach, Surf. Sci. Rep. **29**, 195 (1997).
[2] Rh(100) is a good candidate as a magnetic surface of a nonmagnetic material. The discussion from the theoretical and experimental perspectives can be found in N. Stojić, N. Binggeli, and M. Altarelli, Phys. Rev. B **73**, 100405(R) (2006); A. Goldoni, A. Baraldi, M. Barnaba, G. Comelli, S. Lizzit, and G. Paolucci, Surf. Sci. **454-456**, 925 (2000).
[3] An example is surface melting. A pioneering experimental study can be found in J. W. M. Frenken and J. F. van der Veen, Phys. Rev. Lett. **54**, 134 (1985).
[4] The formation of mesoscopic stress domains has been a topic of interest both theoretically and experimentally within the past two decades. For an early and descriptive study, see the work of O. L. Alerhand, D. Vanderbilt, R. D. Meade, and J. D. Joannopoulos, Phys. Rev. Lett. **61**, 1973 (1988).
[5] P. J. Feibelman, Phys. Rev. B **56**, 2175 (1997).
[6] M. J. Harrison, D. P. Woodruff, J. Robinson, D. Sander, W. Pan, and J. Kirschner, Phys. Rev. B **74**, 165402 (2006).
[7] G. Prévot, B. Croset, A. Coati, Y. Garreau, and Y. Girard, Phys. Rev. B **73**, 205418 (2006).
[8] S. Hong, A. Kara, T. S. Rahman, R. Heid, and K. P. Bohnen, Phys. Rev. B **69**, 195403 (2004).
[9] F. W. C. Boswell, Proc. Phys. Soc., London, Sect. A **64**, 465 (1951); C. R. Berry, Phys. Rev. **88**, 596 (1952).
[10] J. S. Vermaak, C. W. Mays, and D. Kuhlmann-Wilsdorf, Surf. Sci. **12**, 128 (1968); C. W. Mays, J. S. Vermaak, and D. Kuhlmann-Wilsdorf, *ibid.* **12**, 134 (1968).
[11] P. Müller and A. Saúl, Surf. Sci. Rep. **54**, 157 (2004).
[12] B. Croset, Y. Girard, G. Prévot, M. Sotto, Y. Garreau, R. Pinchaux, and M. Sauvage-Simkin, Phys. Rev. Lett. **88**, 056103 (2002).
[13] S. Helveg, W. X. Li, N. C. Bartelt, S. Horch, E. Lægsgaard, B. Hammer, and F. Besenbacher, Phys. Rev. Lett. **98**, 115501 (2007).
[14] J. Massies and N. Grandjean, Phys. Rev. Lett. **71**, 1411 (1993).
[15] S. Müller, A. Kinne, M. Kottcke, R. Metzler, P. Bayer, L. Hammer, and K. Heinz, Phys. Rev. Lett. **75**, 2859 (1995).
[16] J. Fassbender, U. May, B. Schirmer, R. M. Jungblut, B. Hillebrands, and G. Güntherodt, Phys. Rev. Lett. **75**, 4476 (1995).
[17] O. V. Lysenko, V. S. Stepanyuk, W. Hergert, and J. Kirschner, Phys. Rev. Lett. **89**, 126102 (2002).
[18] V. S. Stepanyuk, D. I. Bazhanov, W. Hergert, and J. Kirschner, Phys. Rev. B **63**, 153406 (2001).
[19] R. J. Needs, Phys. Rev. Lett. **58**, 53 (1987).
[20] R. J. Needs and M. J. Godfrey, Phys. Rev. B **42**, 10933 (1990).
[21] A. Locatelli, L. Aballe, T. O. Menteş, M. Kiskinova, and E. Bauer, Surf. Interface Anal. **38**, 1554 (2006).
[22] E. Bauer, Rep. Prog. Phys. **57**, 895 (1994).
[23] T. Engel, H. Niehus, and E. Bauer, Surf. Sci. **52**, 237 (1975).
[24] K. E. Johnson, R. J. Wilson, and S. Chiang, Phys. Rev. Lett. **71**, 1055 (1993).
[25] P. K. Wu, M. C. Tringides, and M. G. Lagally, Phys. Rev. B **39**, 7595 (1989).
[26] M. A. Van Hove and S. Y. Tong, Phys. Rev. Lett. **35**, 1092 (1975).
[27] R. X. Ynzunza *et al.*, Surf. Sci. **459**, 69 (2000).
[28] O. M. Braun and Y. S. Kivshar, *The Frenkel-Kontorova Model: Concepts, Methods, and Applications* (Springer, New York, 2004).
[29] S. Baroni, A. D. Corso, S. de Gironcoli, and P. Giannozzi (http://www.pwscf.org).
[30] O. H. Nielsen and R. M. Martin, Phys. Rev. Lett. **50**, 697 (1983).
[31] J. P. Perdew and A. Zunger, Phys. Rev. B **23**, 5048 (1981).
[32] D. Vanderbilt, Phys. Rev. B **41**, 7892 (1990).
[33] M. Arnold, G. Hupfauer, P. Bayer, L. Hammer, K. Heinz, B. Kohler, and M. Scheffler, Surf. Sci. **382**, 288 (1997).
[34] X. Qian and W. Hübner, Phys. Rev. B **60**, 16192 (1999).
[35] I. G. Batirev, W. Hergert, P. Rennert, V. S. Stepanyuk, T. Oguchi, A. A. Katsnelson, J. A. Leiro, and K. H. Lee, Surf. Sci. **417**, 151 (1998).
[36] G. J. Ackland and M. W. Finnis, Philos. Mag. A **54**, 301 (1986).
[37] M. A. Załuska-Kotur, S. Krukowski, Z. Romanowski, and Ł. A. Turski, Phys. Rev. B **65**, 045404 (2001).
[38] J. C. Buchholz, G.-C. Wang, and M. Lagally, Surf. Sci. **49**, 508 (1975).
[39] We note that for the calculation of the force constants, we increased the kinetic energy cutoff to 50 Ry and the charge density cutoff to 500 Ry.
[40] T. H. K. Barron and M. L. Klein, Proc. Phys. Soc. **85**, 523 (1965).
[41] S. Q. Wu, Z. F. Hou, and Z. Z. Zhu, Solid State Commun. **143**, 425 (2007).
[42] D. Sander, A. Enders, and J. Kirschner, Europhys. Lett. **45**, 208 (1999).
[43] A. M. Rodríguez, G. Bozzolo, and J. Ferrante, Surf. Sci. **289**, 100 (1993); F. R. de Boer, R. Boom, W. C. M. Mattens, A. R. Miedema, and A. K. Niessen, *Cohesion in Metals* (North-Holland, Amsterdam, 1988).
[44] Note that for the stretched slab, the calculated stress value has a large contribution from the bulk of the slab, which cancels out by taking the difference between the two slabs with and without oxygen on the surface.
[45] M. J. Harrison, D. P. Woodruff, and J. Robinson, Surf. Sci. **602**, 226 (2008).